LAPPEENRANTA-LAHTI UNIVERSITY OF TECHNOLOGY LUT

School of Energy Systems

Energy Technology

Nikita Ivanov

SMALL-SCALE GAS TURBINE INTEGRATED HEAT EXCHANGER

Examiners: Associate Professor Dr. Ahti Jaatinen-Värri

               Researcher Petri Sallinen

ABSTRACT

Nikita Ivanov

Small-scale gas turbine integrated heat exchanger

Master's thesis 2020

In this project a recuperator design for a microturbine in development was proposed. Different recuperator geometries were evaluated and suiting type was selected for calculation. Example calculation process and results for recuperator with specific cross section dimensions were provided. Sensitivity analysis of main defining parameters was done. The results of the analysis were discussed and recuperator designs for traditional manufacturing and additive manufacturing were proposed.

CONTENT

LIST OF SYMBOLS

Symbols

D, d	diameter	m	T, t	temperature	°C
F	area	m^2	V	volume	m^3
Gr	Grashof number	-	b	width	m
K	heat transfer coefficient	$\dfrac{W}{m^2K}$	n	number, amount	-
L, l	length	m	p	perimeter	m
m	mass	kg	w	flow velocity	$\dfrac{m}{s}$
Nu	Nusselt number	-	α	convection heat transfer	$\dfrac{W}{m^2K}$
P	pressure	Pa	γ	fold angle	°
Pr	Prandtl number	-	δ	thickness	m
Q	heat transfer	W	η	efficiency	-
q_m	mass flow	$\dfrac{kg}{s}$	λ	heat conductivity	$\dfrac{W}{mK}$
Ra	Rayleigh number	-	ν	kinematic viscosity	$\dfrac{m^2}{s}$
Re	Reynolds number	-	ρ	density	$\dfrac{kg}{m^3}$

Subscripts

air	air flow	hyd	hydraulic
avg	average	in	inner
ch	channel	out	outer
eff	effective	pl	plate
fr	friction	req	required
gas	exhaust gas flow	tot	total
HE	heat exchange	log	logarithmic

Abbreviations

AM	additive manufacturing	EBM	electron-beam melting
SLM	selective laser melting	LPF	laser powder forming

1   INTRODUCTION

The rising demand for decentralized power production incites the development of small scale power producing units. Microturbines, along with reciprocating engines, satisfy this demand. The advantages of microturbines over competing technologies are compact size, small number of moving parts, lover emissions, greater efficiency and opportunity to utilize waste fuel [1]. Certain designs of microturbines can be used in waste heat recovery systems to achieve efficiencies of 80% and higher [1].

Microturbine power unit is comprised of a compressor, combustion chamber, turbine and alternator. In addition to main components a recuperator is usually included in the design to improve total efficiency of the unit.

In unrecuperated turbines compressed air is channeled directly into the combustion chamber where burning process occurs. The average electric efficiency of such turbines is around 15%, but they have simpler construction and are easier to produce and design.

Recuperated designs utilize temperature of the exhaust gas to preheat compressed air before the combustion chamber, which allows lower fuel consumption to achieve the same temperatures before the turbine. Lower fuel consumption with the same power output results in higher total efficiency, which reaches values around 20% - 30% for recuperated turbines. Simulations show that efficiency of 45% can be achieved in certain designs [2].

Recuperator as a gas-gas heat exchanger can be implemented in various forms. Comparison of different heat exchange area geometries is a subject of constant research [3][4][5][6]. The most discussed configuration types are plate, plate-fin, tube-fin, spiral and annular. Heat exchanger itself can be implemented as a standalone part, or can be integrated in the design of the microturbine plant. T100 Turbec microturbine is an example of standalone recuperator design (Figure 1) and Capstone microturbines product line for integrated recuperator design (Figure 2). Certain microturbine applications may be limited to certain choice of recuperator design, but in most cases all types may be applied to considered microturbine with difference in performance. Performance is usually judged by recuperation degree, pressure losses, size and weight of the heat exchanger.
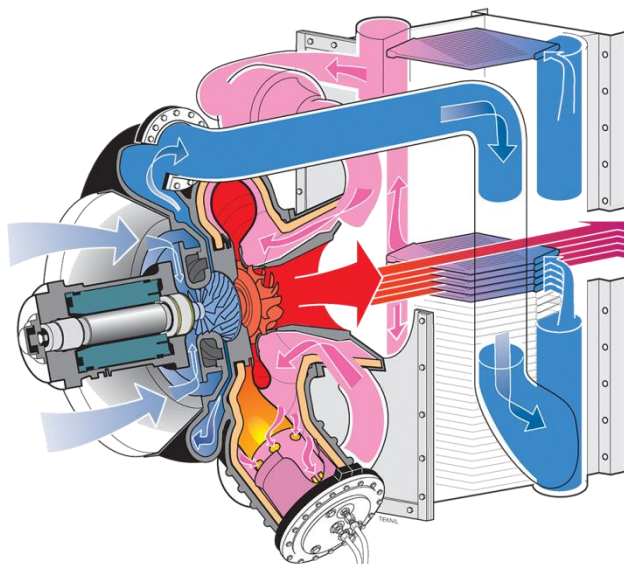
Figure 1. T100 Turbec standalone recuperator. (Source: Turbec Microturbines)
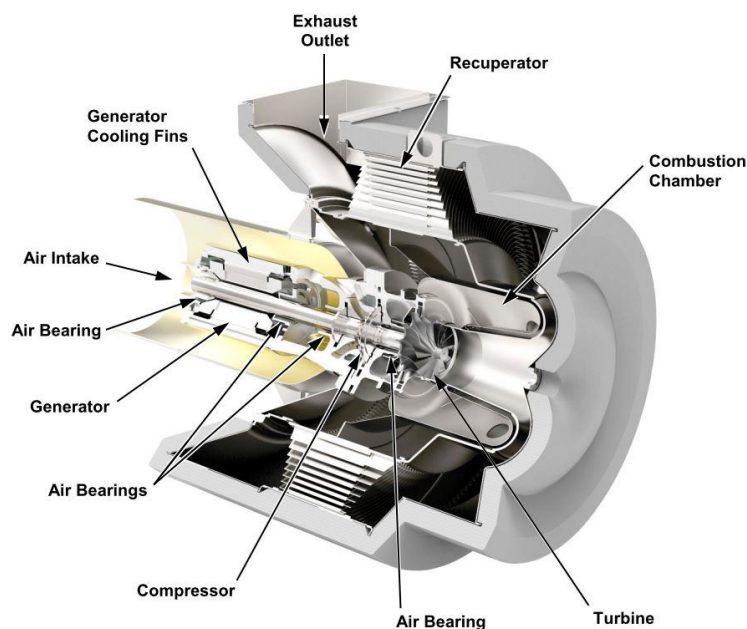

Figure 2. Capstone microturbine integrated recuperator. (Source: Capstone Turbine Corporation)

The aim of this project is to propose a recuperator construction for a microturbine that is being designed by Lappeenranta University of Technology research team. Recuperator must fulfill heat exchange and pressure losses requirements. Additive technologies are considered as production method, which allows achieving certain recuperator construction that cannot be made with traditional production methods. Dimensions and parameters of the turbine are not final and are subject to change. Initial parameters used in the project are discussed further in the designing part.

2   INTEGRATED RECUPERATOR

2.1   Initial data

For this project the plate-fin integrated design similar to Capstone C30 was selected (Figure 3). General form of the recuperator is cylindrical. It is installed as an external housing to the turbine-compressor shaft. Flow channels for air and exhaust gas have axial directions and alternate in counter flow formation.
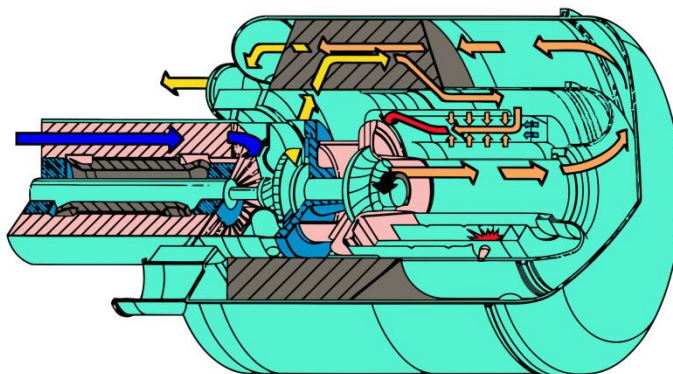

Figure 3. Capstone C30 microturbine [7].

Recuperator is designed for the turbine that is in development, therefore temperature and pressure of acting fluids are subject to change. Parameters of air and exhaust gas, expected by the Lappeenranta University of Technology research team, are presented in the table 1.

Table 1. Parameters of air and exhaust gas for recuperator.

Parameter	Air	Exhaust gas
Inlet temperature, ℃	140	905
Outlet temperature, ℃	831	252
Inlet pressure, bar	4.801	1.022
Outlet pressure, bar	4.705	1.002
Maximum pressure loss, %	2	2
Mass flow, kg/s	0.105	0.106

Important size parameters must be set up before designing integrated solution. The two most important of them are inner and outer diameters of the recuperator. By calculations, they have the biggest impact on the final proportions, weight and cost, but at the same time they are not rigidly fixed or limited by any specific value, therefore they can be a subject of research. Besides inner and outer diameter, other important values, such as channel width, plate thickness and heat

conductivity of the plate may vary in a more limited range, though their impact on the final result should not be underestimated.

In this research no specific goal parameter of a recuperator, such as size, was selected, on the contrary, a variety of solutions is considered and analyzed to identify the advantages and disadvantages of focusing on optimizing specific parameter when dimensioning the heat exchanger. For demonstration purposes, following initial parameters were selected:

Table 2. Initial data for recuperator example calculation.

Parameter	Designation	Value, mm
Inner diameter	D_{in}	250
Outer diameter	D_{out}	500
Channel width	δ_{ch}	3
Plate thickness	δ_{pl}	0.5

The values mentioned in the table 2 above directly define the cross section geometry of the recuperator, except the fins. Further calculations and fin selection reveal the length that a recuperator with such cross section must have to meet the heat exchange requirements.

2.2 General plate geometry

The air and the exhaust gas flow in axial direction in counter flow arrangement. Plates are set in axial plane and are attached to inner and outer sides of the heat exchanger. The distance between the plates defines the width of air and exhaust gas channels. Since the distance between the plates is uniform throughout all the recuperator, the channel geometry for air and gas is the same. Inner diameter defines the inner perimeter of the frame, which defines the amount of plates that can be connected to the frame itself.

Inner perimeter:

$$p_{in} = \pi \cdot D_{in} = \pi \cdot 250 = 785 \text{ mm}$$

The number of channels formed by plates:

$$n_{ch} = \frac{p_{in}}{(\delta_{ch} + \delta_{pl})} = \frac{785}{(3 + 0.5)} = 224.4 = 224$$

$$n_{pl} = n_{ch} = 224$$

Air flow enters the recuperator in radial direction, then turns and flow in axial direction. To minimize pressure losses, plates must be connected to the inner side at 90 degree angle.

However, if the plates are made straight, the channel width between them will not remain uniform throughout the cross section (Figure 4). This is due to the fact that the perimeter of the outer side is larger, and the same number of divisions will lead to a larger gap between the plates.
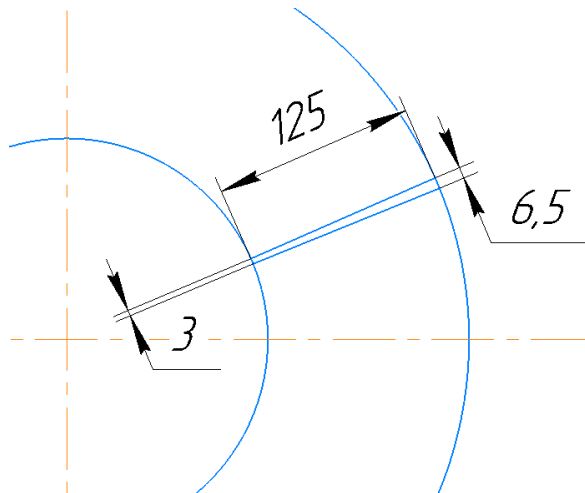

Figure 4. Single channel with straight plates.

Outer perimeter:

$$p_{out} = \pi \cdot D_{out} = \pi \cdot 500 = 1571 \text{ mm}$$

Gap length on outer side of recuperator with straight plates:

$$\delta_{ch,out} = \frac{(p_{out} - n_{pl} \cdot \delta_{pl})}{n_{ch}} = \frac{(1571 - 224 \cdot 0.5)}{224} = 6.5 \text{ mm}$$

To maintain uniform channel width plates must be bent and must attach to the outer side at an angle (Figure 5).
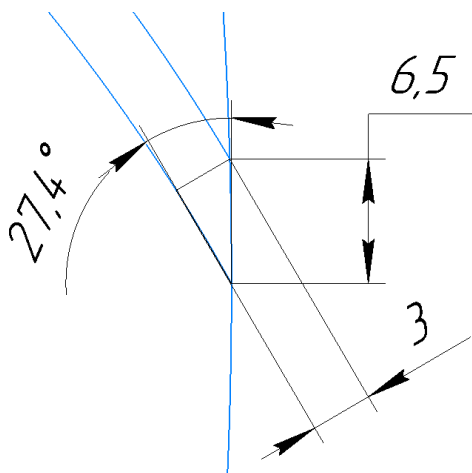

Figure 5. Plate attachment to the outer side.

All plates have the same curvature and the same length, so channel width remains the same between all the plates (Figure 6). Complete cross section is shown in the Figure 7.
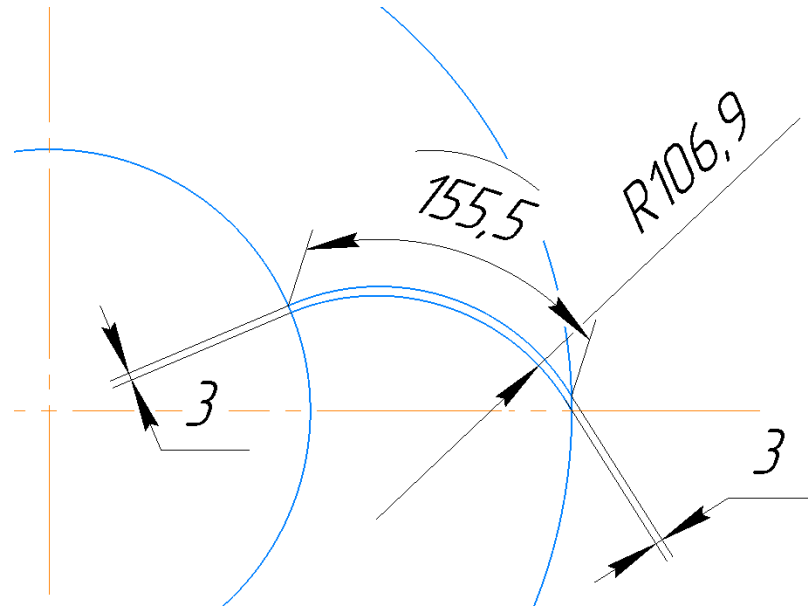

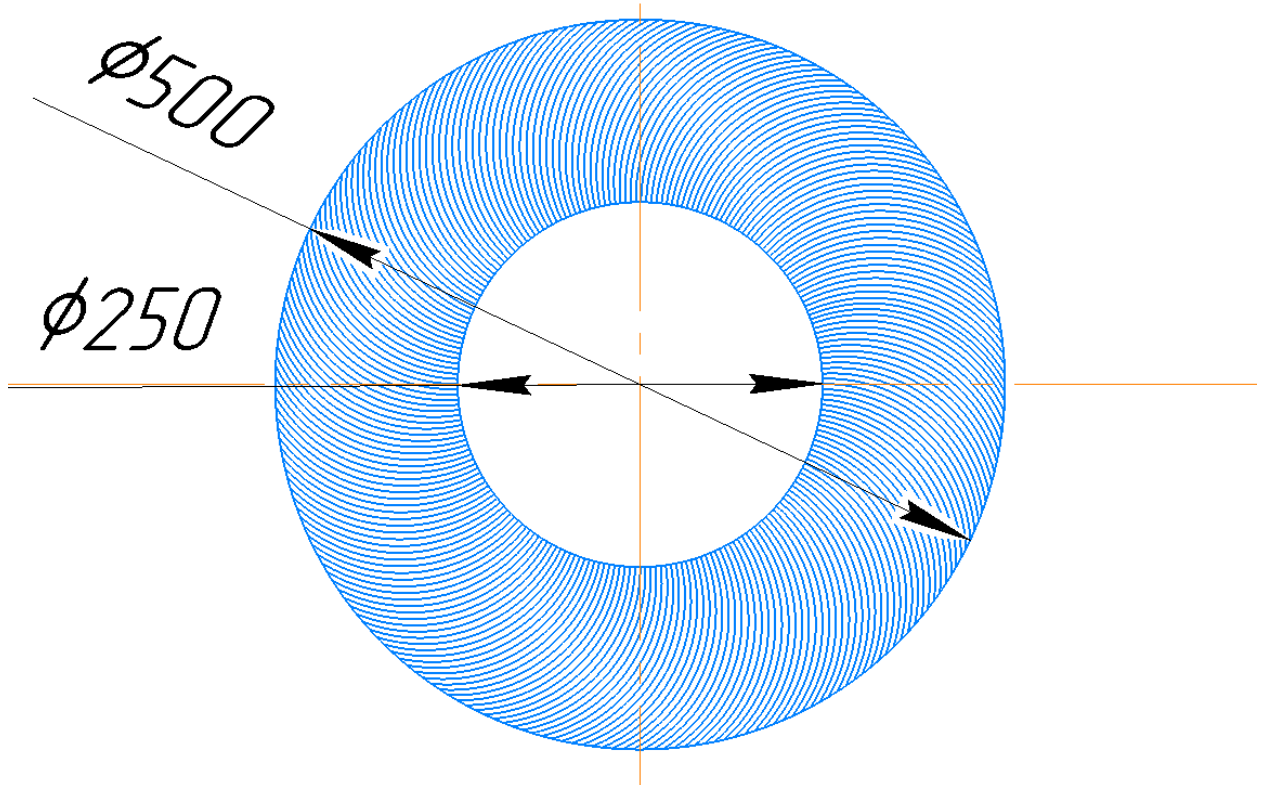**Figure 6.** Single channel with skewed plates.

Figure 7. Cross section of the recuperator without fins.

The resulting value of this stage of designing is the width of a single plate -b_{pl}, which has the value of 155.5 mm from drawing (Figure 6).

2.3   Fin selection

The addition of fins increases the heat exchange area, while at the same time it increases pressure losses and cost of the equipment. They can be implemented in various forms, which suit differently for different heat exchange surfaces.

One of the more suitable fin forms for plate heat exchanger are variations of corrugated sheets. Different corrugated sheet geometries and their heat exchange properties were described by Kays and London [8]. The plate itself can be corrugated, which is one of the most common implementations for simple heat exchangers. In the current example sheet insertion is considered due to higher heat exchange area availability.

Fins in current design are implemented as a corrugated sheet that is inserted into the flow channel in axial direction (Figure 8). The corrugation itself can be realized as a simple bending at a certain degree (90º in this example) or as a wave-shaped bending.
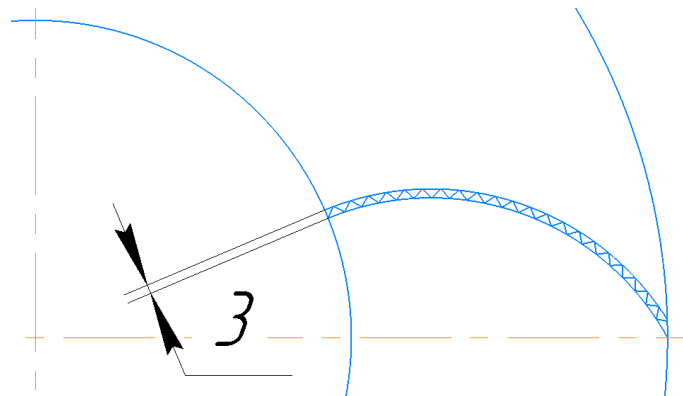

Figure 8. Inserted corrugated sheet.

Such sheets are inserted and welded in each channel. In Figure 9 the recuperator cross section with fins in the air channels is presented. Exhaust gas channels have the same fin insertion but they are not shown in Figure 9 for vision clarity.
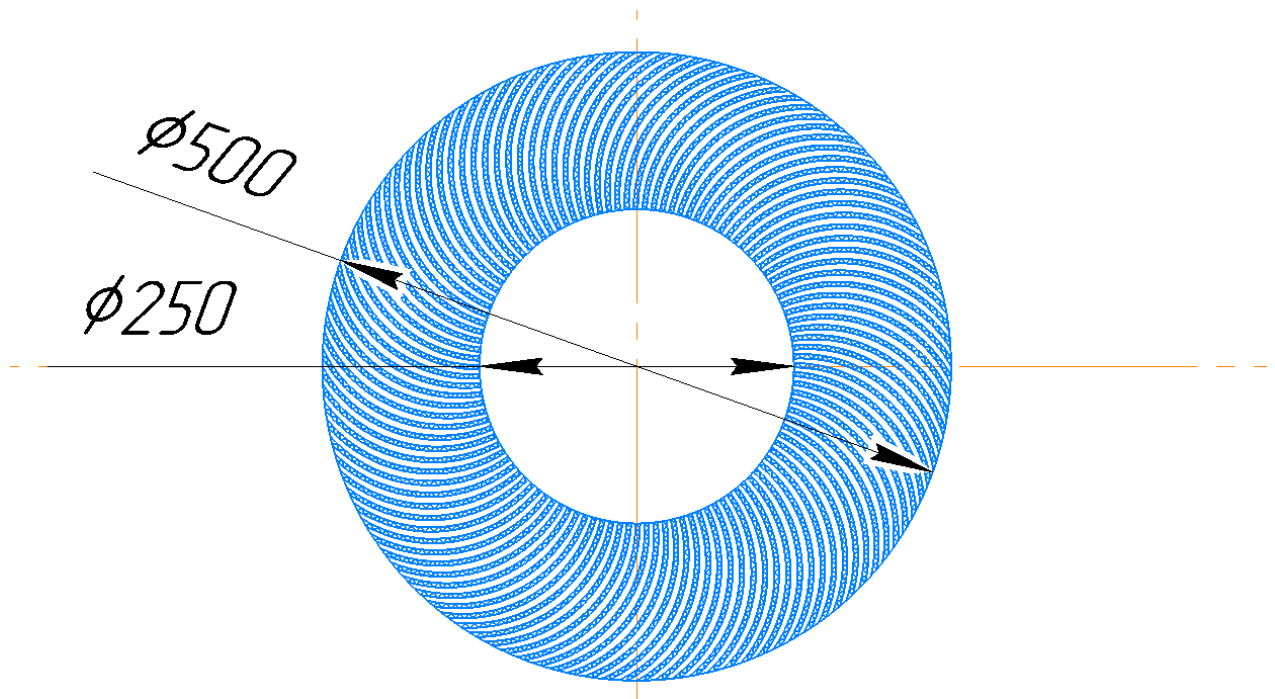
Figure 9. Cross section of the recuperator with fins in air channels.

Corrugated sheets can be made from the same metal as the plates. The thickness of the sheet in combination with heat conductivity affects the efficiency of the added heat exchange surface. The calculation of efficiency is performed later. In this example the thickness of the corrugated sheets was selected equal to the main plates.

Each fold of the sheet can be considered as a separate fin, so the calculation process of a regular fin can be applied. The process and its details are described by Kraus and Aziz [9], and in the following the key aspects of the process are described. First, the length of a fin is calculated as follows:

$$l_{fin} = \frac{\delta_{ch}}{\cos\left(\frac{\gamma_{fold}}{2}\right)} = \frac{3}{\cos\left(\frac{90°}{2}\right)} = 4.2 \text{ mm}$$

And then the number of fins that fit into the channel:

$$n_{fin} = \frac{b_{pl}}{\frac{\delta_{ch}}{\sin\left(\frac{\gamma_{fold}}{2}\right)}} = \frac{155.5}{\frac{4.2}{\sin\left(\frac{90°}{2}\right)}} = 51.8 = 51$$

The fin efficiency calculation uses the value of convection heat transfer coefficient, the calculation of which is shown later. Those two values (η_{fin} and α_{air}) do not affect the calculation of each other. Fin efficiency value is applied in the calculation of the length of the recuperator, which happens after the calculation of the convection heat transfer coefficient. Therefore this value insertion is valid.

Fin efficiency:

$$\varepsilon = \sqrt{\frac{2 \cdot \alpha_{air}}{\lambda_{fin} \cdot \delta_{fin}}} = \sqrt{\frac{2 \cdot 71.15}{25 \cdot 0.0005}} = 106.7$$

$$\eta_{fin} = \frac{\tan(\varepsilon \cdot l_{fin})}{\varepsilon \cdot l_{fin}} = \frac{\tan(106.7 \cdot 0.0042)}{106.7 \cdot 0.0042} = 0.937$$

The efficiency of the fin shows actual contribution of added surface to the heat exchange. Practically it shows how intense the heat exchange on the surface of the fin is compared to the surface of the plate that it is attached to. However, in calculations this effect can be used as an indicator of which part of the fin participates in heat exchange completely and which part does not participate at all. Thus, the non-participating part of the fin is considered only in the flow area and pressure losses calculations.

Effective fin length:

$$l_{fin,eff} = l_{fin} \cdot \eta_{fin} = 4.2 \cdot 0.937 = 4.0 \text{ mm}$$

Effective fin perimeter:

$$p_{fin,eff} = 2 \cdot l_{fin,eff} \cdot n_{fin} = 2 \cdot 4 \cdot 51 = 412 \text{ mm}$$

Wall perimeter is reduced due to the connection points between the sheet and the plate. Effective wall perimeter:

$$p_{pl,eff} = b_{pl} - n_{fin} \cdot \frac{\delta_{fin}}{2\sqrt{2}} = 155.5 - 51 \cdot \frac{0.5}{2\sqrt{2}} = 146.4 \text{ mm}$$

Effective total perimeter:

$$p_{tot,eff} = p_{fin,eff} + p_{pl,eff} = 412 + 146.4 = 558.4 \text{ mm}$$

The value of total effective perimeter is used further to calculate the required length of the plates when the required heat exchange area is found.

Area of the flow channel taken by fins:

$$F_{fin} = n_{fin} \cdot l_{fin} \cdot \delta_{fin} = 51 \cdot 0.0042 \cdot 0.0005 = 0.00011 \text{ m}^2$$

2.4 Heat exchange

The goal of following calculations is to find heat exchange area that suffices the requirements of heat transfer between the air and the exhaust gas. The value of required heat exchange area allows calculation of the length of the recuperator. The cross section of the recuperator that was discussed in previous parts directly defines flow properties and thus heat exchange intensity. First, a total area of the channel that is available for the flow is determined.

Combined flow area:

$$F_{flow,total} = \pi \frac{(D_{out}^2 - D_{in}^2)}{4} - n_{pl} \cdot b_{pl} \cdot \delta_{pl} = \pi \frac{(0.5^2 - 0.25^2)}{4} - 224 \cdot 0.1555 \cdot 0.0005$$

$$= 0.1298 \text{ m}^2$$

Air and exhaust gas channels alternate, so their amount is the same in case of even number of available channels. In case of odd number of available channels, extra channel is allocated to the air flow to minimize pressure losses.

Amount of air channels:

$$n_{ch,air} = \frac{n_{ch}}{2} = \frac{224}{2} = 112$$

Air flow area:

$$F_{flow,air} = F_{flow,total} \frac{n_{ch,air}}{n_{ch}} = 0.1298 \frac{112}{224} = 0.0649 \text{ m}^2$$

The area, occupied by the fins in the channel, is taken into the account in the single channel flow area calculation. Flow area of a single air flow channel (Also equal to the flow area of a single exhaust gas channel):

$$F_{flow,single} = \frac{F_{flow,air}}{n_{ch,air}} - F_{fin} = \frac{0.0649}{112} - 0.00011 = 0.00047 \text{ m}^2$$

Hydraulic diameter of a single channel:

$$d_{hyd} = 4 \cdot \frac{F_{flow,single}}{(\delta_{ch} + \delta_{ch,out} + 2 \cdot b_{pl})} = 4 \cdot \frac{0.00047}{(0.003 + 0.0065 + 2 \cdot 0.1555)} = 0.0059 \text{ m}$$

Air mass flow through one channel:

$$q_{m,air,single} = \frac{q_{m,air}}{n_{ch,air}} = \frac{0.105}{112} = 9.38 \cdot 10^{-4} \frac{\text{kg}}{\text{s}}$$

The velocity of the air flow through one channel:

$$w_{air} = \frac{q_{m,air,single}}{\rho_{air,avg} \cdot F_{flow,single}} = \frac{9.38 \cdot 10^{-4}}{2.164 \cdot 0.00047} = 0.922 \frac{\text{m}}{\text{s}}$$

Reynolds number of the flow:

$$Re_{air} = \frac{w_{air} \cdot d_{hyd}}{v_{air,avg}} = \frac{0.922 \cdot 0.0059}{1.65 \cdot 10^{-5}} = 327$$

The flow is therefore laminar and is far from turbulence. According to Incropera [10] internal laminar flow through the channel between two wide plates can be described with a specific Nusselt number.

$$Nu_{air} = 7.54$$

Convection heat transfer coefficient of the air flow:

$$\alpha_{air} = \frac{Nu_{air} \cdot \lambda_{air,avg}}{d_{hyd}} = \frac{7.54 \cdot 0.0553}{0.0059} = 71.15 \; \frac{W}{m^2K}$$

The calculation process for the exhaust gas flow is the same as for the air flow with the use of respectful values and parameters of the exhaust gas. Important calculation results of the gas flow are listed below:

$$w_{gas} = 4.94 \; \frac{m}{s}$$

$$Re_{gas} = 221$$

$$Nu_{gas} = 7.54$$

$$\alpha_{gas} = 76.76 \; \frac{W}{m^2K}$$

Total heat transfer coefficient from gas to air:

$$K_{total} = \frac{1}{\frac{1}{\alpha_{air}} + \frac{\delta_{pl}}{\lambda_{pl}} + \frac{1}{\alpha_{gas}}} = \frac{1}{\frac{1}{71.15} + \frac{0.0005}{25} + \frac{1}{76.76}} = 36.90 \; \frac{W}{m^2K}$$

Heat transfer calculation requires values of inlet and outlet air (and exhaust gas) temperatures, which are found by iteration process. In this example calculation only the final temperature values are presented. Total heat transfer to the air:

$$Q_{total} = q_{m,air} \cdot C_{p,air,avg} \cdot \left(T_{air}^{outlet} - T_{air}^{inlet}\right) = 0.105 \cdot 1089 \cdot (831 - 140) = 79037$$

Required heat exchange area:

$$F_{heat\;exchange} = \frac{Q_{total}}{K_{total} \cdot \Delta T_{log}} = \frac{79037}{36.90 \cdot 91.64} = 23.37 \; m^2$$

In heat exchange area calculation additional area is above required is usually considered, to counteract the effect of fouling that happens during operation period. Fouling effect can be taken into account by including thermal resistance of fouling layer into total heat exchange coefficient calculation. However, the fouling issue can be addressed also differently. In the current project, a air-gas heat exchanger is calculated with total heat exchange coefficient below 50 W/m2K in all considered cases. For such conditions 2% additional area is recommended by Müller-Steinhagen [11]. This value must be taken into account when the final design of the heat exchanger is calculated, but at the same time its effect on heat exchange and final results is relatively low, when different recuperator designs are compared. Therefore, this area correction value will not be considered in further examples.

The length, that the recuperator with the considered cross section (with fins) must have to satisfy the requirement for the heat exchange area is:

$$L_{req} = \frac{F_{heat\ exchange}}{n_{pl} \cdot p_{tot,eff}} = \frac{23.37}{224 \cdot 0.5584} = 0.187 \text{ m} = 187 \text{ mm}$$

2.5 Pressure losses

Heat exchanger matrix acts as hydraulic resistance to the air and exhaust gas flow and causes the loss of pressure. Lower pressure of the air flow on the turbine inlet corresponds to lower mechanical energy output of the turbine, which means lower total efficiency of the power plant. Therefore heat exchangers are designed to cause as low pressure loss to passing fluids as possible. In this project pressure loss value of 2% for air and exhaust gas is selected as a maximum. Pressure loss calculation for plate heat exchangers is suggested by Leontyev [12].

Friction coefficient for laminar flow:

$$\xi_{fr} = \frac{57}{Re_{air}} = \frac{57}{327} = 0.1955$$

Friction pressure losses:

$$\Delta P_{fr,single} = \xi_{fr} \cdot \frac{w_{air}^2}{2} \cdot \rho_{air,avg} \cdot \frac{L_{req}}{d_{hyd}} = 0.1955 \cdot \frac{0.922^2}{2} \cdot 2.164 \cdot \frac{0.187}{0.0059} = 5.95 \text{ Pa}$$

Inlet properties for each channel:

$$b_{inlet} = \delta_{ch} = 0.003 \text{ m}$$

$$l_{inlet} = 0.05 \text{ m}$$

$$F_{inlet} = b_{inlet} \cdot l_{inlet} = 0.003 \cdot 0.05 = 1.5 \cdot 10^{-4} \text{ m}^2$$

Air flow through the inlet:

$$w_{air,inlet} = \frac{q_{m,air,single}}{\rho_{air,inlet} \cdot F_{inlet}} = \frac{9.38 \cdot 10^{-4}}{4.02 \cdot 1.5 \cdot 10^{-4}} = 1.55 \frac{\text{m}}{\text{s}}$$

Pressure losses at the air inlet:

$$\eta_{inlet} = \frac{F_{inlet}}{F_{flow,single}} = \frac{1.5 \cdot 10^{-4}}{4.7 \cdot 10^{-4}} = 0.32$$

$$\xi_{inlet} = (1 - \eta_{inlet})^2 = (1 - \eta_{inlet})^2 = 0.46$$

$$\Delta P_{inlet,single} = \rho_{air,inlet} \cdot \frac{w_{air,inlet}^2}{2} \cdot (\eta_{inlet}^2 - 1 + \xi_{inlet}) = 4.02 \cdot \frac{1.55^2}{2} \cdot (0.32^2 - 1 + 0.46)$$

$$= -2.11 \text{ Pa}$$

Outlet properties for each channel:

$$b_{outlet} = \delta_{ch} = 0.003 \text{ m}$$

$$l_{outlet} = 0.05 \text{ m}$$

$$F_{outlet} = b_{outlet} \cdot l_{outlet} = 0.003 \cdot 0.05 = 1.5 \cdot 10^{-4} \text{ m}^2$$

$$w_{air,inlet} = \frac{q_{m,air,single}}{\rho_{air,outlet} \cdot F_{outlet}} = \frac{9.38 \cdot 10^{-4}}{1.47 \cdot 1.5 \cdot 10^{-4}} = 4.27 \frac{\text{m}}{\text{s}}$$

$$\eta_{outlet} = \frac{F_{outlet}}{F_{flow,single}} = \frac{1.5 \cdot 10^{-4}}{4.7 \cdot 10^{-4}} = 0.32$$

$$\xi_{outlet} = 0.38$$

$$\Delta P_{outlet,single} = \rho_{air,outlet} \cdot \frac{w_{air,outlet}^2}{2} \cdot (1 - \eta_{outlet}^2 + \xi_{outlet})$$

$$= 1.47 \cdot \frac{4.27^2}{2} \cdot (1 - 0.32^2 + 0.38) = 17.0 \text{ Pa}$$

Total pressure change of air flow through the recuperator:

$$\Delta P_{air} = \left(\Delta P_{inlet,single} + \Delta P_{fr,single} + \Delta P_{outlet,single}\right) \cdot n_{ch} = (-2.11 + 5.95 + 17.0) \cdot 112$$
$$= 2334 \text{ Pa}$$

Relative air pressure drop:

$$\Delta P_{air,\%} = \frac{\Delta P_{total}}{P_{air,inlet}} \cdot 100\% = \frac{2334}{480126} \cdot 100\% = 0.49 \text{ \%}$$

Pressure loss calculation for the exhaust gas flow is the same as for the air flow with the use of respectful parameters of the exhaust gas. Additionally pressure loss from the exhaust tube connection is calculated for the gas side. Total and relative pressure loss of the exhaust gas:

$$\Delta P_{gas} = 27 \text{ Pa}$$

$$\Delta P_{gas,\%} = 0.03 \text{ \%}$$

In this particular example design pressure losses are low for both air and exhaust gas. In the data analysis part of this work it will be shown, that pressure losses may exceed acceptable value with the decrease of the flow area.

2.6   Heat losses

The surface of the recuperator must be insulated to decrease heat loss to surrounding air. Heat losses are proportional to the outer surface of heat exchange equipment, regardless of temperature on the surface, so they can have major effect on heat exchangers of power plants. It will be shown that for a recuperator of a small-scale turbine such losses have negligible effect on the designing process.

The temperature on the surface of the insulation defines heat exchange with surrounding air. Increasing the thickness of the insulation layer leads to lower surface temperature and thus lower heat losses. By calculations, increasing the layer of insulation may satisfy the requirements of heat losses before the temperature on the surface of the insulation becomes low enough to be considered safe for surrounding equipment and personnel. In such cases insulation layer is increased further until the temperature safety requirements are met, otherwise other specific safety measures are implemented.

Surface temperature requirements may differ between countries and industries. For example building codes and regulations in Russia for thermal insulation of equipment and pipelines define maximum acceptable surface temperature of 45 °C for insulated surfaces located in the working or serviced area of premises and containing substances with temperatures above 100 °C [13]. This temperature is selected as goal surface temperature for all heat loss calculations further in the project.

Multiple insulation variants are available for high temperature conditions with specific limitations [14]. When the condition of 45 °C surface temperature is to be met, heat losses do not depend on the properties of selected insulation. Therefore any insulation suitable for current application can be used. For this example calculation Promalight-1000X was selected as insulation with heat conductivity of 0.03 W/mK in 600 °C temperature area. Calculations show that a layer of 150 mm meets the surface temperature requirement.

Average temperature on the recuperator outer surface:

$$T_{HE,surface,avg} = \frac{T_{air,avg} + T_{gas,avg}}{2} = \frac{485.5 + 578.5}{2} = 532 \ °C$$

Temperature on inner surface of insulation:

$$T_{ins,inner} = T_{HE,surface,avg} - \Delta t_{HE|ins} = 532 - 5 = 527 \ °C$$

Assumed temperature difference between outer surface of insulation and surrounding air temperature:

$$\Delta t_{ins|air} = 25 \ °C$$

Outer surface temperature:

$$T_{ins,outer} = T_{room} + \Delta t_{ins|air} = 20 + 25 = 45 \ °C$$

Grashof number:

$$Gr = \frac{g \cdot \beta \cdot (T_{ins,outer} - T_{room}) \cdot L_{sp}^{\;3}}{\nu_{room}^{\;2}} = \frac{9.81 \cdot 0.00312 \cdot (45 - 20) \cdot (2 \cdot 0.15 + 0.8)^3}{(1.506 \cdot 10^{-5})^2} =$$

$$= 1.73 \cdot 10^9$$

Rayleigh number:

$$Ra = Gr \cdot Pr_{room} = 1.73 \cdot 10^9 \cdot 0.678 = 1.17 \cdot 10^9$$

Churchill and Chu [15] recommend following correlation for Nusselt number calculation for horizontal cylinder:

$$Nu = \left[0.60 + \frac{0.387 \cdot Ra^{1/6}}{\left[1 + \left(\frac{0.559}{Pr} \right)^{9/16} \right]^{8/27}} \right]^2 = \left[0.60 + \frac{0.387 \cdot (1.17 \cdot 10^9)^{1/6}}{\left[1 + \left(\frac{0.559}{0.678} \right)^{9/16} \right]^{8/27}} \right]^2 = 120.85$$

Heat transfer coefficient to outside air:

$$\alpha_{convection} = \frac{Nu \cdot \lambda_{room}}{L_{sp}} = \frac{120.85 \cdot 0.0259}{2 \cdot 0.15 + 0.5} = 3.91 \; \frac{W}{m^2 K}$$

Total heat transfer coefficient:

$$K_{convection} = \frac{1}{\dfrac{1}{\alpha_{convection}} + \dfrac{L_{ins}}{\lambda_{ins}}} = \frac{1}{\dfrac{1}{3.91} + \dfrac{0.15}{0.03}} = 0.19 \; \frac{W}{m^2 K}$$

Surface area with insulation:

$$F_{ins,total} = \pi \cdot (2 \cdot L_{ins} + D_{out}) \cdot L_{req} = \pi \cdot (2 \cdot 0.15 + 0.5) \cdot 0.187 = 0.470 \; m^2$$

General heat loss:

$$Q_{loss} = K_{convection} \cdot F_{ins,total} \cdot (T_{ins,inner} - T_{room}) = 0.19 \cdot 0.470 \cdot (527 - 20) = 45 \; W$$

Actual temperature of the outer layer of the insulation:

$$T_{ins,outer} = T_{ins,inner} - \frac{Q_{loss} \cdot L_{ins}}{F_{ins,total} \cdot \lambda_{ins}} = 527 - \frac{45 \cdot 0.15}{0.470 \cdot 0.03} = 44.66 \; °C$$

Relative heat loss:

$$Q_{loss,\%} = \frac{Q_{loss}}{Q_{total}} \cdot 100\% = \frac{45}{79037} \cdot 100\% = 0.06 \; \%$$

2.7 Compactness coefficient

Compactness coefficient describes how much heat exchange area is fit into volume taken by heat exchanger. Different types of heat exchange geometries with the same provided heat exchange area result in different volume taken by the equipment. Without consideration of application

field, shell and tube heat exchangers, for example, take more space than plate heat exchangers with the same heat exchange area available, therefore the latter are considered more compact.

Heat exchanger volume:

$$V_{HE} = \pi \frac{D_{out}^2}{4} L_{req} = \pi \frac{0.5^2}{4} 0.187 = 0.037 \text{ m}^3$$

Compactness coefficient:

$$\varepsilon_{HE} = \frac{F_{heat\ exchange}}{V_{HE}} = \frac{23.37}{0.038} = 637 \frac{\text{m}^2}{\text{m}^3}$$

Typical values of compactness coefficient for different geometries are presented in the table 3.

Table 3. Compactness of different heat exchange geometries [12].

Heat exchange geometry	Compactness, $\frac{\text{m}^2}{\text{m}^3}$
Smooth tube	400
Plate	600
Finned tube	800
Finned plate	1800
Porous and mesh	9000

2.8   Weight of the recuperator

Weight of the recuperator not only indicates the mechanical load that it provides to the structure, but represents the cost of steel used in assembly. Thus, when comparing different designs of the recuperator, the design with the lowest mass can be considered the least expensive to produce.

Cross section area of the plates:

$$F_{cs,plates} = n_{pl} \cdot \delta_{pl} \cdot b_{pl} = 224 \cdot 0.0005 \cdot 0.1555 = 0.0174 \text{ m}^2$$

Cross section area of the fins:

$$F_{cs,fins} = n_{ch} \cdot \delta_{fin} \cdot l_{fin} \cdot n_{fin} = 224 \cdot 0.0005 \cdot 0.0042 \cdot 51 = 0.0246 \text{ m}^2$$

Volume of steel used in the recuperator:

$$V_{steel} = (F_{cs,plates} + F_{cs,fins}) \cdot L_{req} = (0.0174 + 0.0246) \cdot 0.187 = 7.86 \cdot 10^{-3} \text{ m}^3$$

Weight of the recuperator:

$$m_{steel} = \rho_{steel} \cdot V_{steel} = 7800 \cdot 7.86 \cdot 10^{-3} = 61.3 \text{ kg}$$

3 DATA ANALYSIS

3.1 Outer diameter variation

The change of inner and outer diameters of the recuperator determines the majority of other parameters and final dimensions of the heat exchanger. Therefore, a sensitivity analysis is done.

First the impact of the outer diameter is considered. Seven designs of the recuperator with variable outer diameters were calculated. All designs have the same parameters and dimensions as were selected for the example calculation earlier in the paper, except the outer diameter of the recuperator. Cross sections of the considered designs are represented in the Figure 10.

Calculations show, that the increase of outer diameter results in shorter length of the recuperator and lower pressure and heat losses (Figure 11). Outer diameter does not affect the total amount of channels in the recuperator, so its variation only leads to the increase of the flow area of both exhaust gas and air. Bigger flow area of the channel results in the increase of heat exchange area available per meter, which leads to the decrease of the length of the heat exchanger. Pressure losses directly depend on the flow area and channel length; therefore they have similar dynamics of change (Figure 11).

The change of the compactness coefficient is represented in the Figure 12. The change of weight of the recuperator is shown in the Figure 13.
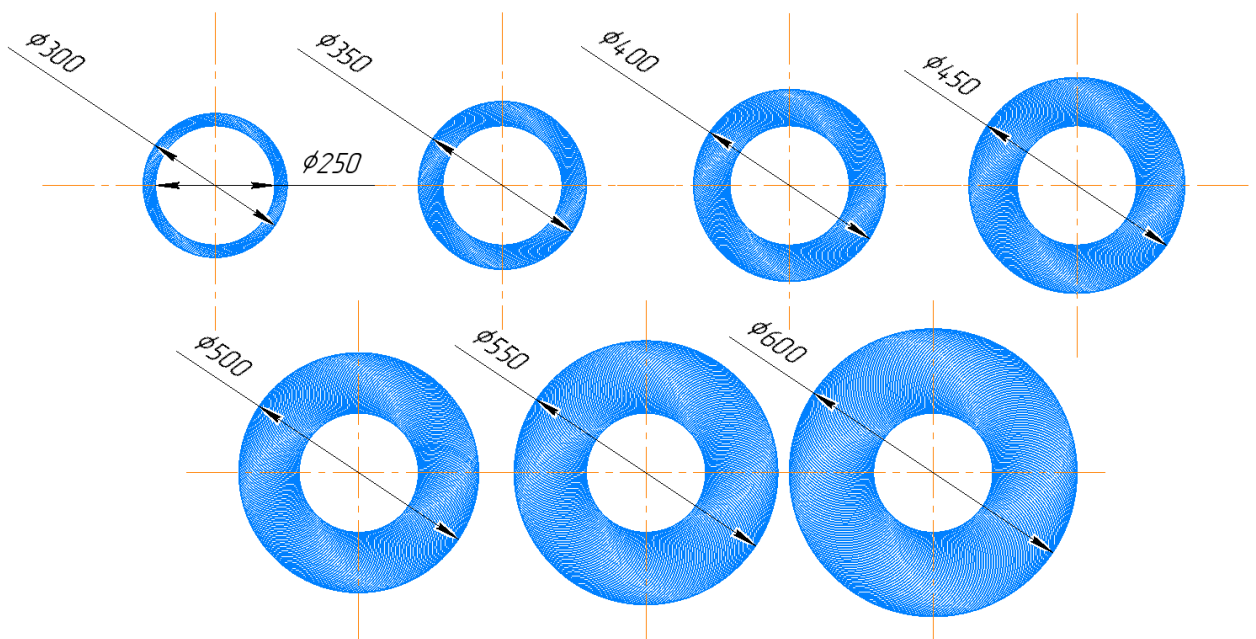

Figure 10. Cross sections of the considered designs with $D_{in} = 250$ mm and different D_{out}.
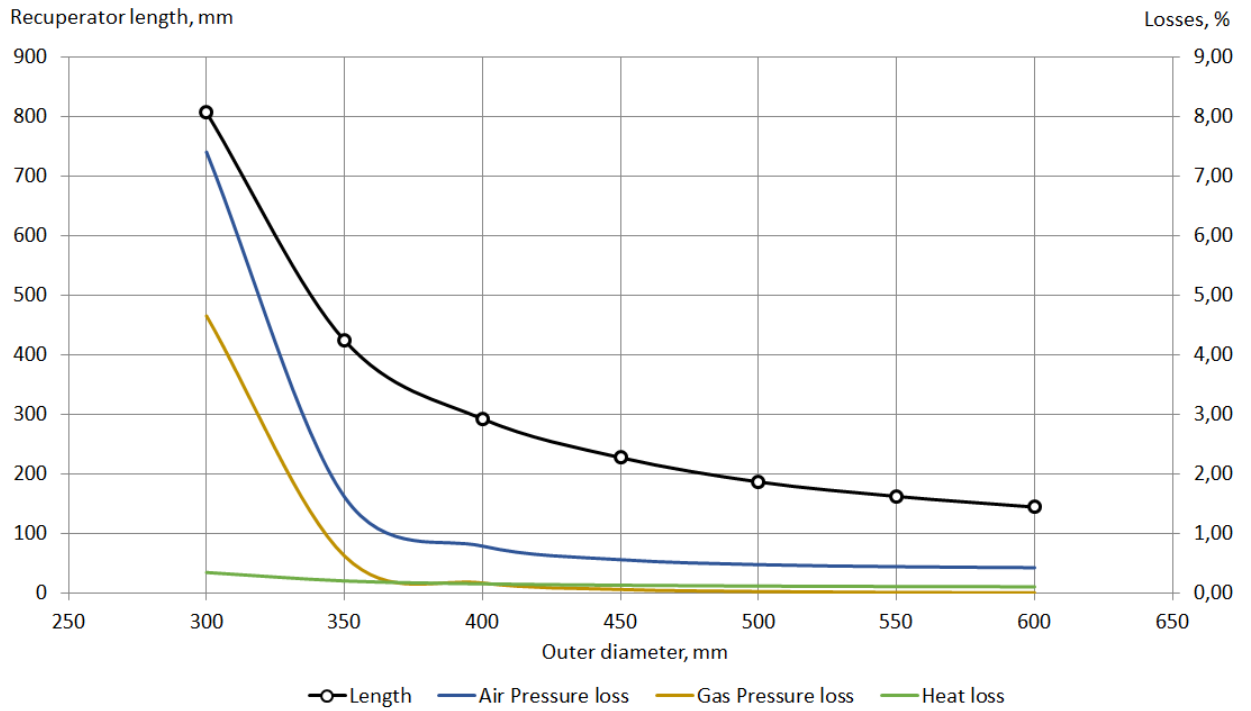
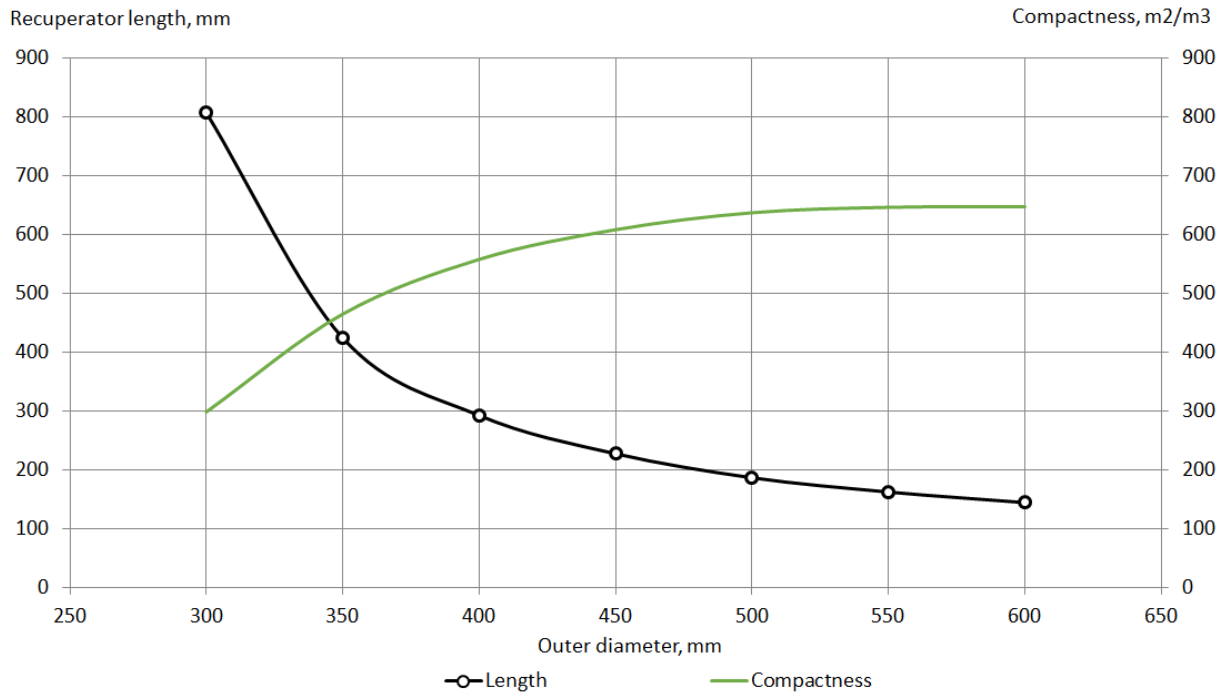**Figure 11.** Recuperator length and losses vs. outer diameter of the recuperator.

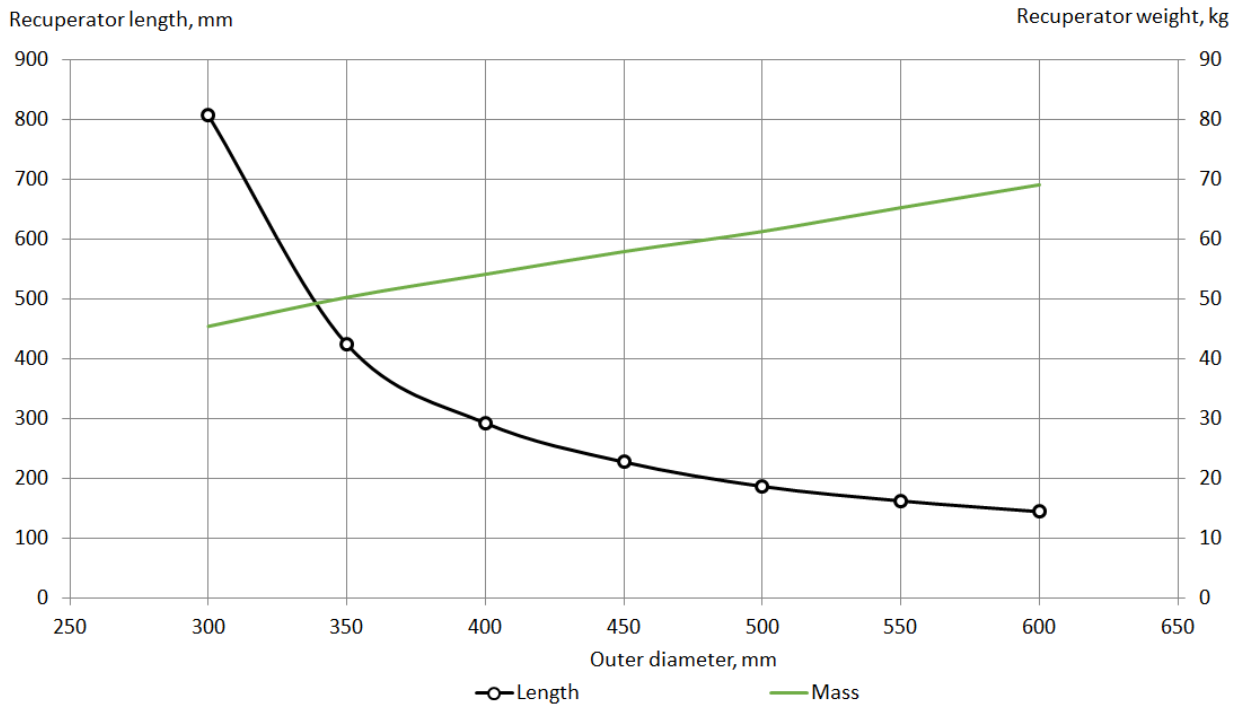**Figure 12.** Recuperator length and compactness vs. outer diameter of the recuperator.

Figure 13. Recuperator length and weight vs. outer diameter of the recuperator.

3.2 Inner diameter variation

Second group of considered designs have the same outer diameter of 500 mm but various inner diameter. Cross sections of the considered designs are presented in Figure 14. Length and losses calculation results are presented in Figure 15.

The relationship, shown in Figure 15, indicates that there are limitations to the way the recuperator length can be controlled by changing the inner diameter. With the increase of the inner diameter, total length decreases only to a certain value and then rises back. This is explained by two different changes that are connected to the inner diameter value.

Inner diameter directly defines the amount of channels that can be connected to the inner side of the recuperator. Thus, bigger inner diameter leads to the higher amount of flow channels, which leads to more fin insertion, therefore increasing heat exchange area available per meter. At the same time bigger inner diameter results in lesser width of the flow channel, which in the end results in the decrease of heat exchange area available per meter. At a certain value of inner diameter these counteracting effects become equal in the impact they deal, thus defining the minimum value of the recuperator length.

The change of the compactness coefficient is represented in the Figure 16. The change of weight of the recuperator is shown in the Figure 17.
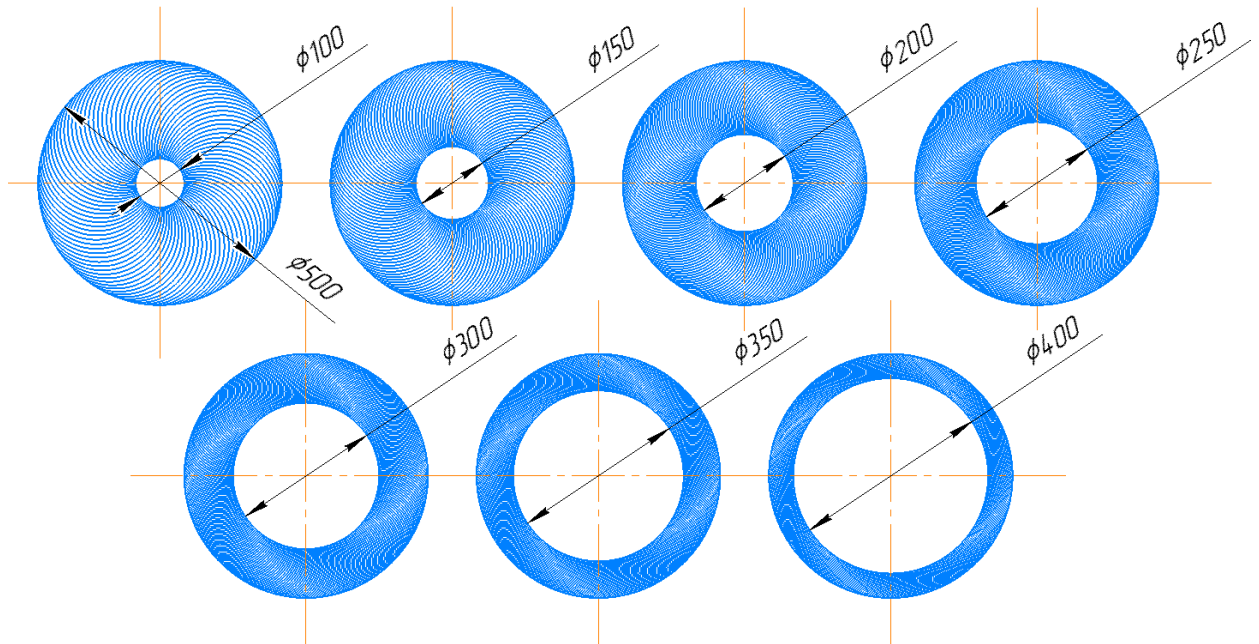

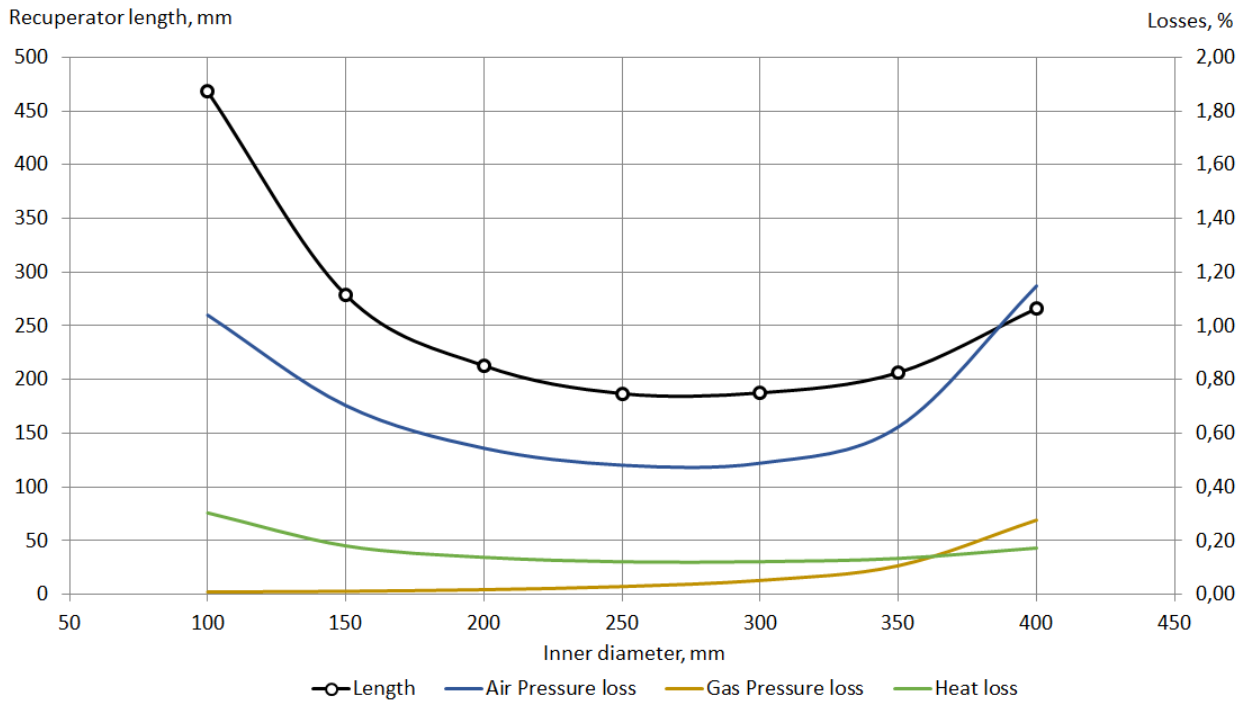**Figure 14.** Cross sections of the considered designs with $D_{out} = 500$ mm and different D_{in}.

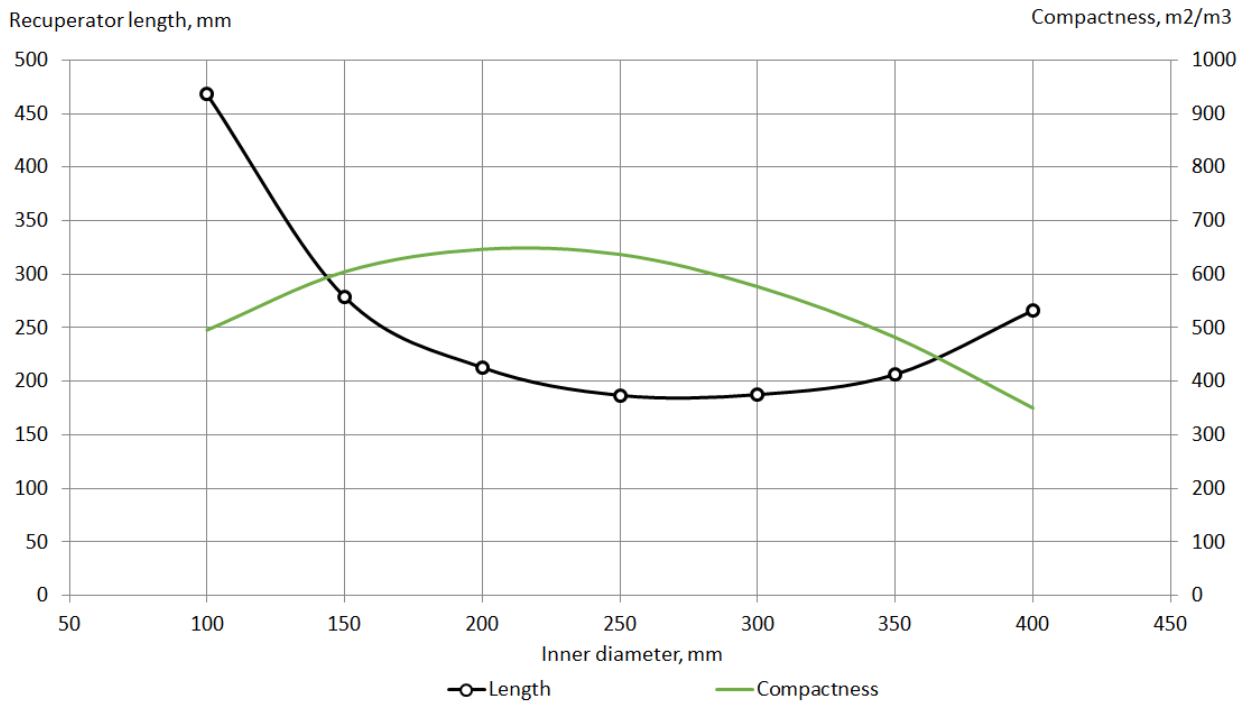**Figure 15.** Recuperator length and losses vs. inner diameter of the recuperator.

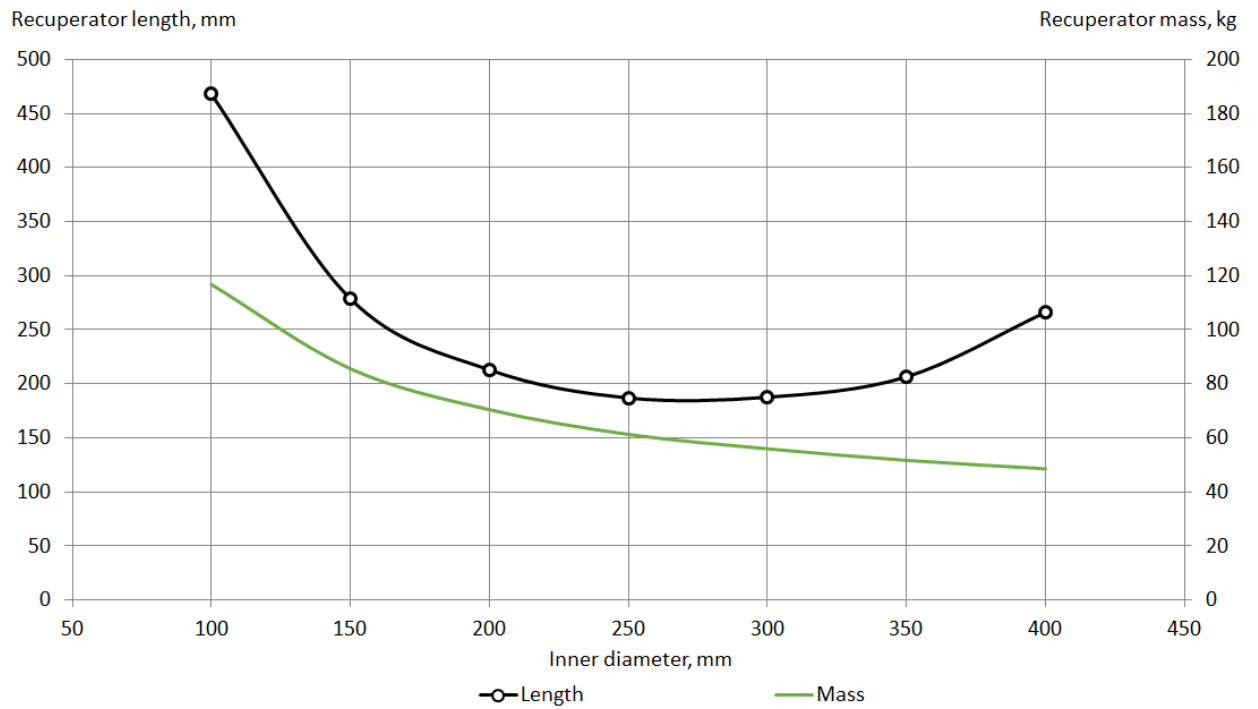**Figure 16.** Recuperator length and compactness vs. inner diameter of the recuperator.

Figure 17. Recuperator length and weight vs. inner diameter of the recuperator.

3.3   Fin geometry variation

The choice of fins, in addition to the choice of diameters, has a significant impact on the final size of the heat exchanger. It must be noted, that in case, when a particular corrugated sheet finning cannot be applied due to technology limitations, a substitute sheet geometry can be used to achieve similar heat exchange. Moreover, various fin geometries can be used to meet heat exchange requirements in cases when dimension parameters such as outer or inner diameters are confined in a narrow range of values.

To demonstrate that, three different sheet geometries are considered and calculated. First one is of the same type that was presented in all of the calculations before - corrugated sheet with folds at a specific angle, but with the angle reduced to 35 degree instead of 90 degrees. Second geometry has smooth folds that form wavy structure of the sheet. Third geometry has structure of the square wave. Cross sections of channel with the considered sheet variants are presented in the Figure 18.
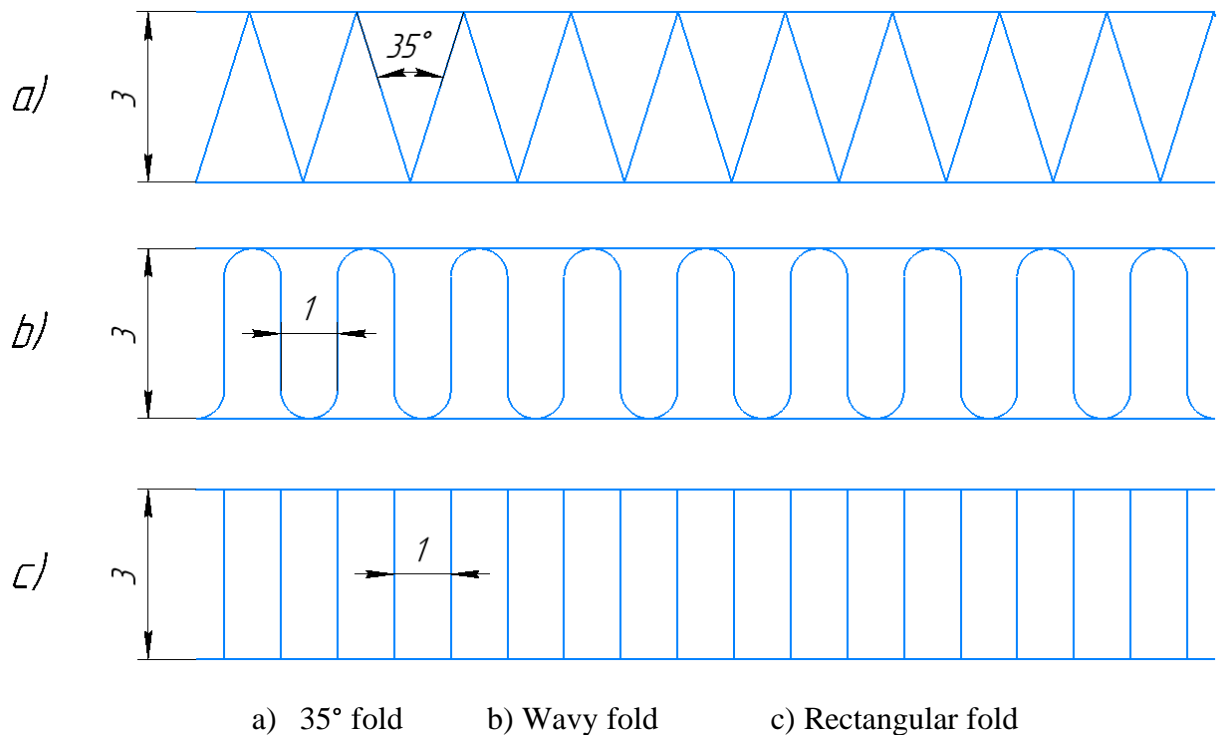

a)   35° fold   b) Wavy fold   c) Rectangular fold

Figure 18. Corrugation variants of the inserted sheets.
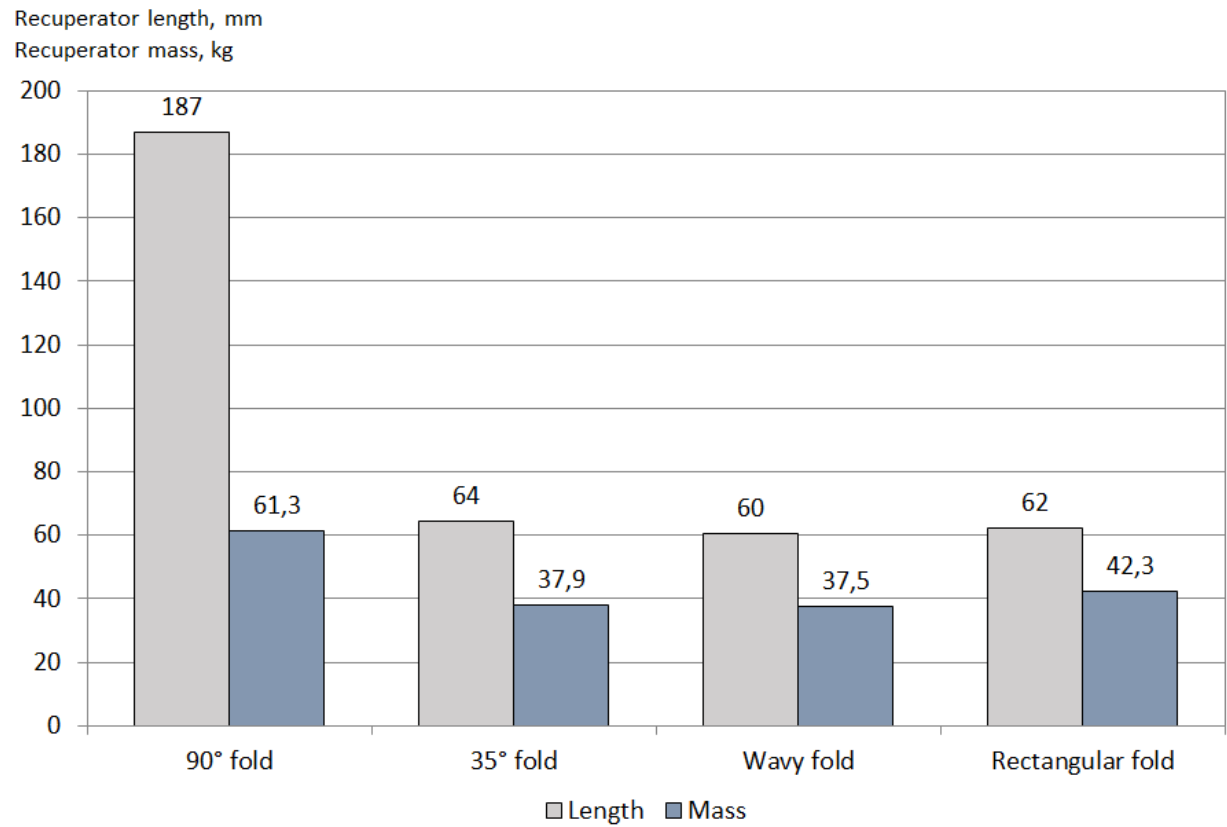
Recuperator length, mm
Recuperator mass, kg

Figure 19. Length and mass of the designs with different fin geometry.

Calculations show that similar result can be achieved with different fin geometries (Figure 19). The length of the recuperator can be varied by choice of fin geometry, when other dimensions cannot be changed to achieve required heat exchange values.

4   ADDITIVE MANUFACTURING TECHNOLOGY

The term "Additive manufacturing" (AM) describes processes of creating objects through consequent material accretion. Current advances in this field allow production from various materials, such as polymers, thermoplastics, metal alloys and ceramics. The term 3D-printing usually refers to technologies of nonmetal materials, which are becoming widely available for commercial use. Production from metals, however finds more and more applications in industry.

The driving force for additive manufacturing from metals originates from aerospace and medical industries. Latest investigations in high temperature stainless steel, titanium and nickel alloys reveal the potential for small-sized heat exchange equipment with a complex structure that could not be created with use of traditional technologies. Multiple AM technologies are available for metal alloy production.

Selective Laser Melting (SLM) is a technique designed to use high power-density laser to melt and fuse metallic powders. The SLM method is also known as direct selective laser sintering, LaserCusing, and direct metal laser sintering, and it has been proven to produce parts up to 99.9% relative density [16]. Small material particles in form of powder are placed in a powder bed and selectively fused on the surface by the laser after scanning cross-sections of 3-D model (Figure 20).
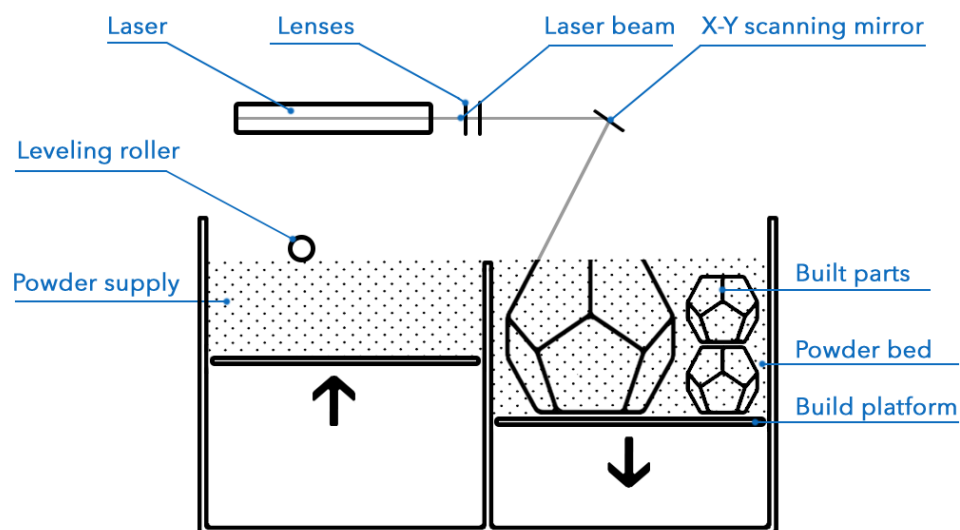

Figure 20. SLM production method.

Electron-beam melting (EBM) is a process of material fusing in vacuum with use of computer-controlled electron beam. This technique is distinct from SLM as the raw material (metal powder or wire) fuses having completely melted (Figure 21).
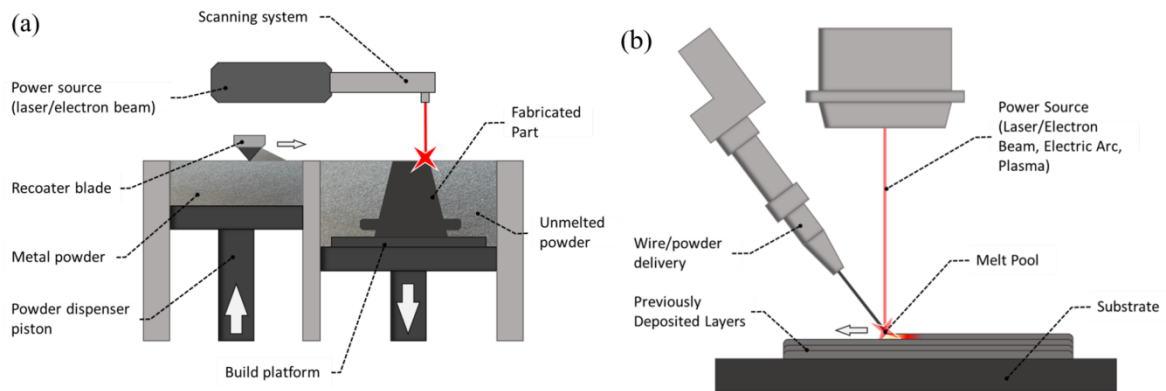

Figure 21. EBM production method. (a – with powder, b – with wire)

Laser powder forming (LPF) uses metal powder injected into a molten pool that is created by a focused, high-powered laser beam to create objects from 3D models. Powder nozzle and laser head are usually implemented as one piece, so printing volume is only limited to the reach of robot guiding arm (Figure 22). Objects created with this technology can be substantially larger than with technologies that use powder beds, such as SLM.
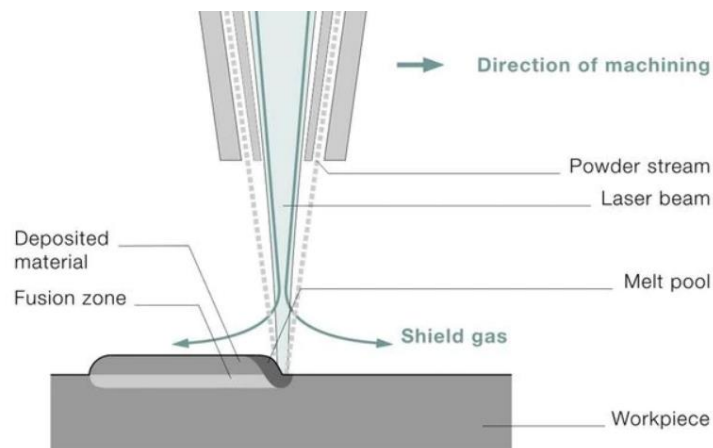

Figure 22. LPF production method.

Those technologies have specific limitations, cost and quality, but they provide promising solutions to high temperature heat exchanger production. Various materials are already used in production of recuperators with the use of AM, such as Inconel 625, Inconel 718, ABD®-900AM, CM 247LC and SS316 L [17]. Material choice and production methods are subject of cost calculation that is not a part of this project.

5   PROPOSED DESIGN

Recuperated heat exchanger results with Traditional and Additive manufacturing are presented in this section. Considering all parameter and sizing variations, fin and material selection, optimal recuperator solutions for both technologies are proposed.

Selected inner diameter provides enough channels for heat exchange and leaves space inside for the turbo unit, combustion chamber and structural elements. Outer diameter in combination with fin selection provides enough flow area for required heat exchange and acceptable pressure losses. The recuperator length is commensurate with the diameter, which makes the design compact. The resulted compactness coefficient of 1205 shows efficient heat exchange area placement inside the recuperator. As a result, the weight is reduced to 59.1 kg. Such design can be realized with traditional technology with all the elements produced separately and welded together.

Close cross section view of air channels is presented in Figure 23. The comparison cross section view of the design from example calculation and the proposed design is presented in Figure 24. All defining dimension values of traditional design are presented in the table 4. Heat exchange parameters and pressure losses are presented in the table 5.

 When applying additive manufacturing method, multiple adjustments can be made to improve the design. Channel width can be decreased due to absence of welding limitations. Corrugated sheet insertion is printed as part of the main plate so wavy fold geometry can be replaced by rectangular fold with the same spacing to simplify the mesh and provide more structural integrity to the cross section. If the provided advantages of additive manufacturing are taken, weight of the recuperator can be reduced from 59.1 to 24.7 kg and length from 286 mm to 136 mm with pressure losses still in the acceptable range.

The comparison cross section view of air channels and all channels is presented in Figure 25. All defining dimension values of additive manufacturing design are presented in the table 4 and compared with results for traditional design. Heat exchange parameters and pressure losses are presented in the table 5.
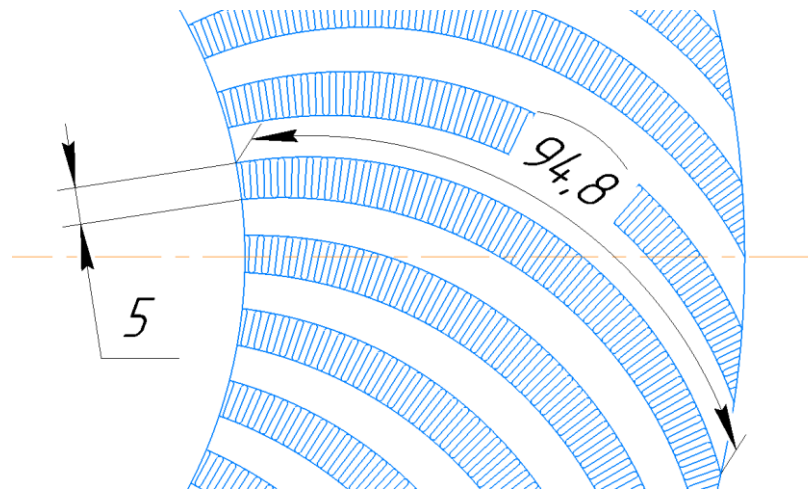
Figure 23. Air channel cross section of traditional design.
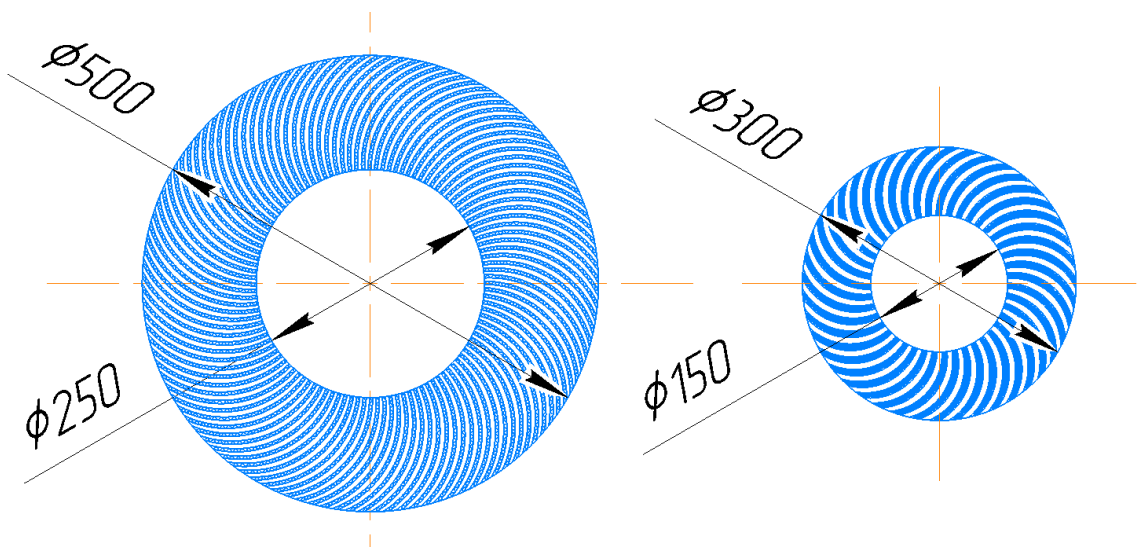

Figure 24. Cross sections of the traditional design from example calculation (left) vs. final design (right).
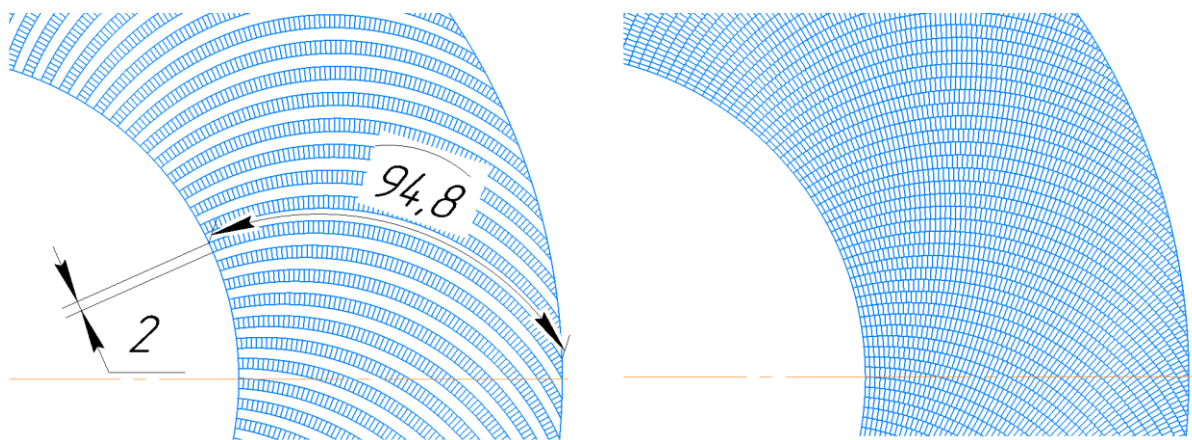

Figure 25. Cross section of additive manufacturing design.

(Air channels only – left, all channels – right.)

Table 4. Dimensions of proposed designs.

Parameter	Traditional design	AM
Inner diameter, mm	150	150
Outer diameter, mm	300	300
Length, mm	286	136
Number of plates	85	204
Plate skew radius, mm	64.2	64.2
Plate thickness, mm	0.5	0.3
Channel gap, mm	5	2
Channel width, mm	94.8	94.8
Air channels	43	102
Exhaust gas channels	42	102
Fin insertion type	Wavy fold	Straight fin
Sheet thickness, mm	0.5	0.3
Spacing between each fold, mm	1	1

Table 5. Performance parameters of proposed designs.

Parameter	Traditional design	AM
Total heat exchange area, m^2	24.3	11.9
Total heat transfer coefficient, $\frac{W}{m^2 K}$	35.5	72.5
Total heat transfer, kW	79.0	79.0
Average air flow velocity, $\frac{m}{s}$	3.61	3.25
Average exhaust gas flow velocity, $\frac{m}{s}$	19.8	17.4
Air pressure loss, kPa	2.24	8.59
Relative air pressure loss, %	0.47	1.79
Exhaust gas pressure loss, kPa	0.64	0.36
Relative exhaust gas pressure loss, %	0.63	0.36
Compactness coefficient, $\frac{m^2}{m^3}$	1205	1235
Weight, kg	59.1	24.7

6   CONCLUSIONS

Microturbine technology was evaluated. Different recuperator geometries were compared and suiting type was selected for calculation. Important defining parameters were discussed and process of calculation with example values was presented. Multiple recuperator designs were calculated and analyzed.

Analysis shows that variation of defining recuperator dimensions leads to specific changes of final design and performance. Increase of outer diameter results in shorter length of the recuperator and lower pressure losses and vice versa. Variation in inner diameter of the recuperator results in length change behavior with local minimum. Thus, the length cannot be adjusted below a certain value when inner diameter is changed. Fin insertion is important part of heat exchange intensification. It was shown than fin geometries are interchangeable and that recuperator performance can be enhanced with denser fin insertion.

Traditional and additive manufacturing (AM) technologies were evaluated and different production methods were compared. Based on the sensitivity analysis, recuperator designs for traditional manufacturing and additive manufacturing were proposed. It was shown that with the same radial dimensions of the recuperator AM design has lower length and mass, due to lower obtainable flow area of flow channels, which can reduce the manufacturing cost significantly.

The results of this project demonstrate benefits of designing heat exchange equipment with additive manufacturing technologies. Future developments in this field may contribute to wider spread of AM in industry and replace equipment parts in traditional design with lighter, smaller and potentially cheaper AM counterparts.

LIST OF LITERATURE

[1] Capehart. B. L. 2016. "Microturbines". Whole Building Design Guide. National Institute of Building Sciences.

[2] Malkamäki M., et al. 2015. "A HIGH EFFICIENCY MICROTURBINE CONCEPT". 11th European Conference on Turbomachinery Fluid Dynamics and Thermodynamics.

[3] McDonald C. F. 2003. *Recuperator considerations for future higher efficiency microturbines*. Appl Therm Eng 23(12):1463–1487.

[4] Ji Hwan Jeong, et al. 2007. "Review of Heat Exchanger Studies for High-Efficiency Gas Turbines". ASME Turbo Expo 2007: Power for Land, Sea, and Air.

[5] Utriainen E., Sunden B. 1998. *Recuperators in gas turbine systems*. ASME Turbo Expo, 98-GT-165.

[6] Foerster S. and Kleeman M. 1978. *Compact metallic and ceramic recuperators for gas turbines*. ASME Paper 78-GT-62.

[7] Capstone Turbine Corporation [official website] Available at: www.capstoneturbine.com; Path: Products – C30. Date: 01.09.2020.

[8] Kays W., London A. 1998. *Compact Heat Exchangers*. 3rd ed. McGraw-Hill.

[9] Kraus A., Aziz A., 2002. *Extended Surface Heat Transfer*. John Wiley & Sons

[10] Incropera F., Bergman T., DeWitt D., Lavine A. 2007. *Fundamentals of Heat and Mass Transfer*. 6th ed. John Wiley & Sons.

[11] Müller-Steinhagen H. 2000. *Heat Exchanger Fouling: Mitigation and Cleaning Techniques*. IChemE.

[12] Leontyev A. I. 2004. *Heat exchangers and cooling systems for gas turbine and combined plants*. [In Russian] Moscow: 2nd ed. Publishing house of MSTU.

[13] SNiP 2.04.14-88. Thermal insulation of equipment and pipelines / Gosstroy of Russia. - Moscow: TsITP Gosstroy USSR, 1998. - 28 p.

[14] Wilk J., Gil P., Tychanicz-Kwiecień M. 2018. Review of High-Temperature Thermal Insulation Materials. Journal of Thermophysics and Heat Transfer 33(11):1-13.

[15] Churchill S. W. and Chu H. H. S. 1975. Correlating Equations for Laminar and Turbulent Free Convection from a Horizontal Cylinder. International Journal of Heat and Mass Transfer, 18, 1049-1053.

[16] Chor Yen Yap; et al. 2015. Review of selective laser melting: Materials and applications. Applied Physics Reviews 2(4):041101.

[17] HiETA Technologies Ltd. [official website] Available at: www.hieta.biz; Path: Products – High-Temperature Compact Heat Exchangers. Date: 01.09.2020.